International Journal of Mechanical and Materials Engineering (IJMME), Vol. 5 (2010), No. 1, 18-28.

MIXED CONVECTION ANALYSIS IN TRAPEZOIDAL CAVITY WITH A MOVING LID

M.A.H. Mamun[1], T.R. Tanim[2], M.M. Rahman[3], R. Saidur[4] and S. Nagata[1]

[1]Institute of Ocean Energy, Saga University, 1 Honjo-machi, Saga 840-8502, Japan
[2]Mechanical Engineering Department, Ohio University, Athens, OH-45701, USA
[3]Department of Mathematics,
Bangladesh University of Engineering and Technology (BUET), Dhaka-1000, Bangladesh
[4]Department of Mechanical Engineering, University of Malaya, 50603 Kuala Lumpur, Malaysia
E-mail: hasan@ioes.saga-u.ac.jp

ABSTRACT

Mixed convection heat transfers in a two-dimensional trapezoidal cavity with constant heat flux at the heated bottom wall while the isothermal moving top wall in the horizontal direction has been studied numerically. Control Volume based finite volume method (FVM) has been used to discretize the governing differential equations. The pressure- velocity coupling in the governing equations is achieved by using the well known SIMPLE method for numerical computations. A second order upwind differencing scheme is to be used for the formulation of the coefficients in the finite-volume equations. All computations are to be done for a range of Richardson number, *Ri* from 0.1 to 10 and the aspect ratio, *A* are to be changed from 0.5 to 2 for a fluid having Prandtl number equal to 0.71 (air). First the optimum configuration of the trapezoidal cavity has been obtained by changing the inclination angle, γ of the side walls. Then the effect of Richardson number, aspect ratio, and Rotation angle, Φ (30°, 45° and 60°) of the optimum trapezoidal cavity has been studied by changing the desired parameter. Results have been presented in the form of streamline and isotherm plots as well as the variation of the Nusselt number at the heat source surface under different conditions. The results shows that with increasing *Ri*, the heat transfer rate increases as natural convection dominates. The rotational angle of the trapezoidal cavity and the direction of the lid motion affect the heat transfer rate significantly. Optimum heat transfer rate is obtained at aiding flow condition having higher values of *Ri*.

Keywords: Mixed convection, Trapezoidal cavity, lid-driven cavity, Finite volume method.

NOMENCLUTURE

h	convective heat transfer coefficient (W/m^2 K)
q''	Heat Flux (W/m^2)
C_P	specific heat at constant pressure (J/kg K)
g	gravitational acceleration (m/s^2)
k	thermal conductivity of the fluid (W/m K)
Nu	Nusselt number, hW/k
Pr	Prandtl number, ν/α
Gr	Grashof number, $g\beta\Delta TW^3/\nu^2$
Re	Reynolds number, U_0W/ν
Ri	Richardson number, Gr/Re^2
A	Aspect Ratio, H/W
R	length of the inclined sidewalls (m)
T	temperature of the fluid , (^oC)
u	velocity component at x-direction (m/s)
U	dimensionless velocity component at X-direction
v	velocity component at y-direction (m/s)
V	dimensionless velocity component at Y-direction
W	length of the cavity, (m)
x	distance along the x-coordinate
X	distance along the non-dimensional x-coordinate
Y	distance along the non-dimensional y-coordinate

Greak Symbols

α	thermal diffusivity of the fluid (m^2/s)
β	volumetric coefficient of thermal expansion (K^{-1})
γ	inclination angle of the sidewalls of the cavity
θ	dimensionless temperature ,$(T_H-T_C)/\Delta T$
μ	dynamic viscosity of the fluid (Pa s)
ν	kinematic viscosity of the fluid (m^2/s)
ρ	density of the fluid (kg/m^3)
Φ	rotational angle of the cavity

Subscripts

av	average value
c	value of cold temperature
H	value of hot temperature

1. INTRODUCTION

Flow and heat transfer analysis in lid-driven cavities is one of the most widely studied problems in thermo-fluids area. Numerous investigations have been conducted in the past on lid-driven cavity flow and heat transfer considering various combinations of the imposed temperature gradients and cavity configurations. This is because the driven cavity configuration is encountered in many practical engineering and industrial applications. Such configurations can be idealized by the simple rectangular geometry with regular boundary conditions yielding a well-posed problem. Combined forced-free convection flow in lid-driven cavities or enclosures occurs as a result of two competing mechanisms. The first is due to shear flow caused by the movement of one of the walls of the cavity while the second is due to buoyancy flow produced by thermal non homogeneity of the cavity boundaries. Understanding these mechanisms is of great significance from technical and engineering standpoints.

Air-cooling is one of the preferred methods for the cooling of computer systems and other electronic equipments, due to its simplicity and low cost. It is very important that such cooling systems should be designed in the most efficient way and the power requirement for the cooling should be minimized. The electronic components are treated as heat sources embedded on flat surfaces. A small fan blows air at low speeds over the heat sources. This gives rise to a situation where the forced convection due to shear driven flow and the natural convection due to buoyancy driven flow are of comparable magnitude and the resulting heat transfer process is categorized as mixed convection. Mixed convection flow and heat transfer also occur frequently in other engineering and natural situations. One important configuration is a lid-driven (or shear- driven) flow in a differentially heated/cooled cavity, which has applications in crystal growth, flow and heat transfer in solar ponds [Cha and Jaluria (1984)], dynamics of lakes [Imberger and Hamblin (1982)], thermal-hydraulics of nuclear reactors [Ideriah (1980)] , industrial processes such as food processing, and float glass production [Pilkington (1959)]. The interaction of the shear driven flow due to the lid motion and natural convective flow due to the buoyancy effect is quite complex and warrants comprehensive analysis to understand the physics of the resulting flow and heat transfer process.

There have been many investigations in the past on mixed convective flow in lid-driven cavities. Many different configurations and combinations of thermal boundary conditions have been considered and analyzed by various investigators. Aydin and Yang (2000) numerically studied mixed convection heat transfer in a two-dimensional square cavity having an aspect ratio of 1. In their configuration the isothermal sidewalls of the cavity were moving downwards with uniform velocity while the top wall was adiabatic. A symmetrical isothermal heat source was placed at the otherwise adiabatic bottom wall. They investigated the effects of Richardson number and the length of the heat source on the fluid flow and heat transfer. Shankar et al. (2002) presented analytical solution for mixed convection in cavities with very slow lid motion. The convection process has been shown to be governed by an inhomogeneous biharmonic equation for the stream function. Oztop and Dagtekin (2004) performed numerical analysis of mixed convection in a square cavity with moving and differentially heated sidewalls. Sharif (2007) investigates heat transfer in two-dimensional shallow rectangular driven cavity of aspect ratio 10 and Prandtl number 6.0 with hot moving lid on top and cooled from bottom. They investigated the effect of Richardson number and inclination angle. Guo and Sharif (2004) studied mixed convection in rectangular cavities at various aspect ratios with moving isothermal sidewalls and constant heat source on the bottom wall. They plotted the streamlines and isotherms for different values of Richardson number and also studied the variation of the average Nu and maximum surface temperature at the heat source with Richardson number with different heat source length. They simulated streamlines and isotherms for asymmetric placements of the heat source and also the effects of asymmetry of the heating elements on the average Nu and the maximum source length temperature. Basak et.al. (2010) numerically studied the mixed convection flows in a lid-driven square cavity filled with porous medium by using penalty finite element analysis for uniformly heated bottom wall, linearly heated side walls or cooled right wall. They found that average Nusselt numbers are almost invariant with Gr for low Pr with all Darcy number for linearly heated side walls or cooled right wall.

In the present paper two dimensional steady, mixed convection heat transfers in a two-dimensional trapezoidal cavity with constant heat flux from heated bottom wall while the isothermal moving top wall has been studied numerically. The present study is based on the configuration of Aydin and Yang (2000) where the isothermal heat source at the bottom wall is replaced by a constant flux heat source, which is physically more realistic. The main attribute for choosing the trapezoidal shape cavity is to enhance the heat transfer rate as it could be said intuitionally due to its extended cold top surface. The inclination angle of the sidewalls of the trapezoid has been changed (30°, 45° and 60°) to get the maximum heat transfer in terms of maximum Nusselt number. Then the trapezoid has been rotated (30°, 45° and 60°) and the results have been studied. The tilted position of the enclosure shows a significant influence on the heat transfer. Results are obtained for both the aiding and opposing flow conditions by changing the direction of the lid motion. This study includes additional computations for cavities at various aspect ratios, *A*, ranging from 0.5 to 2 and their effects on the heat transfer process is analyzed in terms of average Nusselt number. Contextually the present study will focus on the computational analysis of the influence of inclination angle of the sidewalls of the cavity, rotational angle of the cavity, Aspect ratio, direction of the lid motion and Richardson number.

2. PHYSICAL MODEL

The physical model considered here is shown in figure 1 and 2, along with the important geometric parameters. It consists of a trapezoidal cavity filled with air, whose bottom wall and top wall are subjected to hot T_H and cold T_C temperatures respectively while the side walls are kept adiabatic. Two cases of thermal boundary conditions for the top moving wall have been considered here. The first case is (figure 1) when the moving cold wall is moving in the positive x direction (opposing flow condition). In that case the shear flow caused by moving top wall opposes the buoyancy driven flow caused by the thermal non-homogeneity of the cavity boundaries. The second case is (figure 2) when the moving cold wall is moving in the negative x direction (aiding flow condition). In that case the shear flow assists the buoyancy flow. The cavity height is H, width of the bottom hot wall is W, is inclined at angle Φ with the horizontal reference axis. γ is the inclination angle of the sidewalls of the cavity. The flow and heat transfer phenomena in the cavity are investigated for a series of Richardson numbers (Ri), aspect ratio (A=H/W), rotation angle of the cavity Φ.

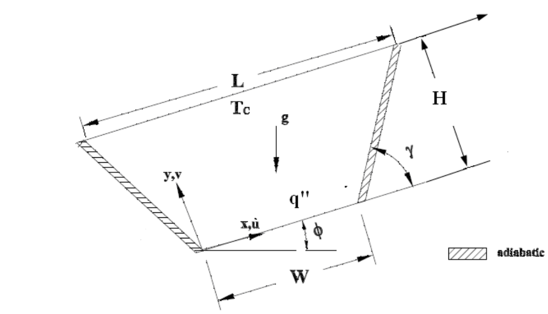

Figure 1: Schematic diagram of the physical system considering opposing flow condition

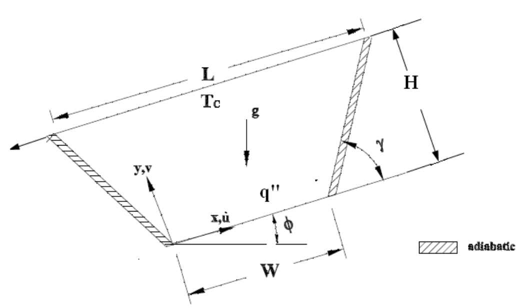

Figure 2: Schematic diagram of the physical system considering aiding flow condition

2.1 Mathematical Model

Using the Boussinesq approximation and neglecting the viscous dissipation effect and compressibility effect the dimensionless governing equations for two dimensional laminar incompressible flows can be written as follows:

$$\frac{\partial U}{\partial X}+\frac{\partial V}{\partial Y}=0 \qquad (1)$$

$$U\frac{\partial U}{\partial X}+V\frac{\partial U}{\partial Y}=-\frac{\partial P}{\partial X}+\frac{1}{\mathrm{Re}}\left(\frac{\partial^2 U}{\partial X^2}+\frac{\partial^2 U}{\partial Y^2}\right) \qquad (2)$$

$$U\frac{\partial V}{\partial X}+V\frac{\partial V}{\partial Y}=-\frac{\partial P}{\partial Y}+\frac{1}{\mathrm{Re}}\left(\frac{\partial^2 V}{\partial X^2}+\frac{\partial^2 V}{\partial Y^2}\right)+\frac{Gr}{\mathrm{Re}^2}\theta \qquad (3)$$

$$U\frac{\partial \theta}{\partial X}+V\frac{\partial \theta}{\partial Y}=\frac{1}{\mathrm{Re}\,\mathrm{Pr}}\left(\frac{\partial^2 \theta}{\partial X^2}+\frac{\partial^2 \theta}{\partial Y^2}\right) \qquad (4)$$

The dimensionless variables are as follows:

$X=x/W$, $Y=y/W$, $\theta=(T_H-T_C)/\Delta T$, $\Delta T=q''W/k$, $U=u/U_0$, $V=v/U_0$, $P=p/\rho U_o^2$

The dimensionless parameters, appearing in Eqs. (1)-(4) are Reynolds number $Re= U_0W/v$, the Prandtl number $Pr=v/\alpha$, the Grashof number $Gr=\frac{g\beta\nabla TL^3}{v^2}$. The ratio of Gr/Re^2 is the mixed convection parameter and is called Richardson number *Ri* and is a measure of the relative strength of the natural convection and forced convection for a particular problem. If *Ri*<<1 the forced convection is dominant while if *Ri*>> 1, then natural convection is dominant. For problems with *Ri*~1 then the natural convection effects are comparable to the forced convection effects.

The boundary conditions for the present problem are specified as follows:

Top wall: $U=U_0$, $V=0$, $\theta=0$
Bottom wall: $U=V=0$, $\theta=1$
Right and Left wall: $U=V=0$, $\partial\theta/\partial X=0$

Non-dimensional heat transfer parameter Nusselt number is stated as:

$$Nu_{av}=\int_0^W \frac{h(x)x}{k}dx$$

$$Nu_{av}=\int_0^1 \left(\frac{\partial \theta}{\partial Y}\right)_{Y=0} dX$$

2.2 Numerical Method

Firstly the problem is defined as a two dimensional enclosure. Control Volume based finite volume method (FVM) is to be used to discretize the governing differential equations. The pressure- velocity coupling in the governing equations is achieved using the well known SIMPLE method for numerical computations. The set of governing equations are to be solved sequentially. A second order upwind differencing scheme is to be used for the formulation of the coefficients in the finite-volume equations. As the sides of the trapezoidal cavity are not parallel, the present numerical techniques will descretize the computational domain into unstructured triangular elements.

In order to obtain the grid independence solution, a grid refinement study is performed for the trapezoidal cavity (A=1) under constant heat flux condition keeping, Re=400, Pr=0.71, Ri= 1.0.n It is found in figure 3 that 5496 regular nodes are sufficient to provide accurate results. This grid resolution is therefore used for all subsequent computations for A≤1. For taller cavities with A>1, a proportionately large number of grids in the vertical direction is used.

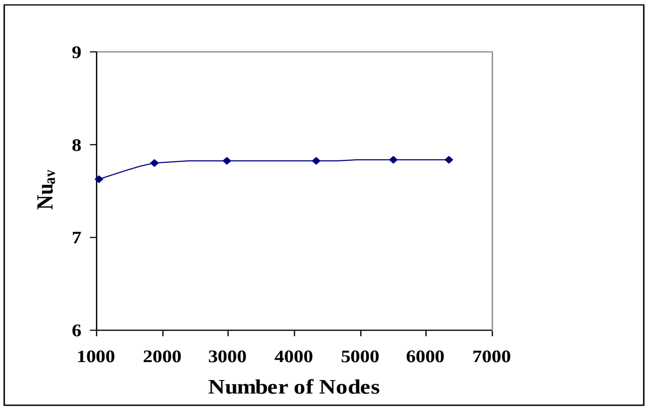

Figure 3: Grid sensitivity test for Trapezoidal cavity at Ri=1.0, Re=400 and A=1.

The convergence criterion was defined by the required scaled residuals to decrease 10^{-5} for all equations except the energy equations, for which the criterion is 10^{-8}.

The computational procedure has been validated against the numerical results of Guo and Sharif (2004) shown in the figure 4.

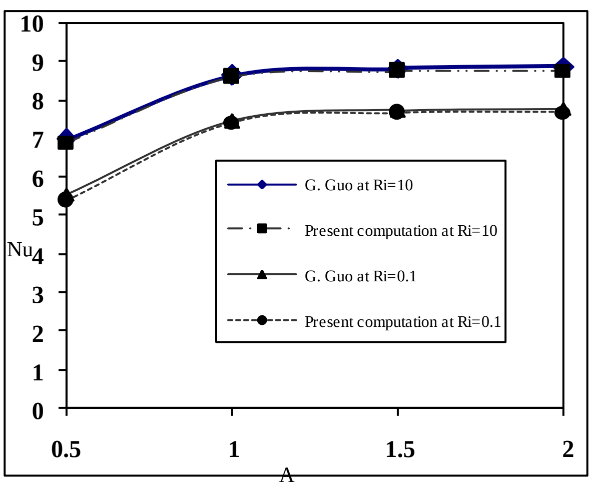

Figure 4: Variation of the Average Nusselt number with different Aspect Ratio at Ri=10, Re=100 and ε =0.6

Figure 4, reveals that the Average Nusselt numbers in the present study have excellent agreement with those obtained by Guo and Sharif (2004) having a maximum discrepancy of about 2.3% Therefore, it can be concluded that the numerical code used in this analysis can solve the present problem with reasonable agreement.

3. RESULTS AND DISSCUSSION

Numerical results are presented in order to determine the effects of the inclination angle of the side walls, Richardson number *Ri*, Reynolds number *Re*, Aspect ratio *A*, the rotational angle of the cavity *Φ* on mixed convection flow in trapezoidal enclosure. The inclination angle of the sidewalls of the trapezoidal enclosure has been changed from 30º to 60º with an interval of 15º. The values of Richardson number varies from 0.1 to 10, Aspect ratio, *A* changes from 0.5 to 2.0 taking Rotational angle 30º, 45 º, 60º for two different Reynolds numbers 400 and 600.

3.1 Effect of Inclination Angle

In this study the effect of inclination angle of the adiabatic sidewalls has been observed first. The inclination angle of the side walls has been changed to 30º, 45 º and 60º. The Richardson number has been changed from 0.1 to 10. The optimum inclination angle has been selected based on the average Nusselt number which is a non dimensional parameter that indicates the rate of heat transfer between the hot and cold walls. The results are obtained both for *Re*=400 and *Re*=600.

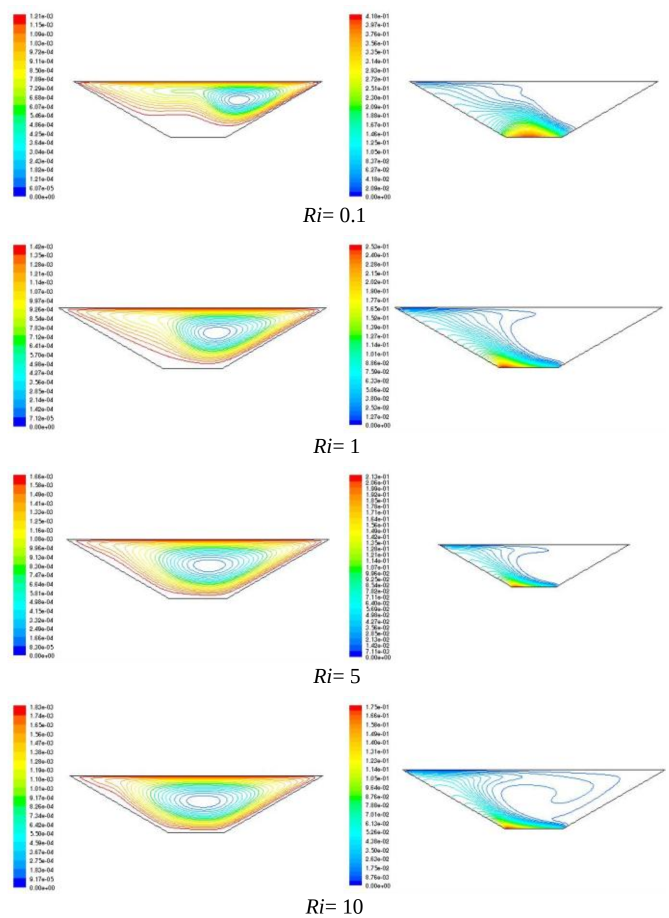

Figure 5: Contours of Streamlines and isotherms at Re=400, A=1.0 and γ=30°

Figure 5-7 reveals the impact of varying inclination angles of the sidewalls of the trapezoidal cavity. These figures show the contours of streamlines and isotherms at different Richardson numbers. For small values of *Ri* number, it can be seen that the shear effect due to the movement of the top wall is dominant. The fluid flow is characterized by a primary re-circulating eddy of the size of the cavity generated by the movement of the top lid. The isothermal contour maps are clustered near the bottom and top walls resulting in steep temperature gradient there. In each case as the Richardson number increases the convection current becomes more dominant resulting in stronger flow field. Again at γ=45º (figure 6), the flow field is stronger than the γ=30º and γ=60º (figure 5 and figure 7), which is an indication of better heat transfer. The isothermal plots also complies with the flow field, showing minimum value of the maximum isotherms at γ=45º.

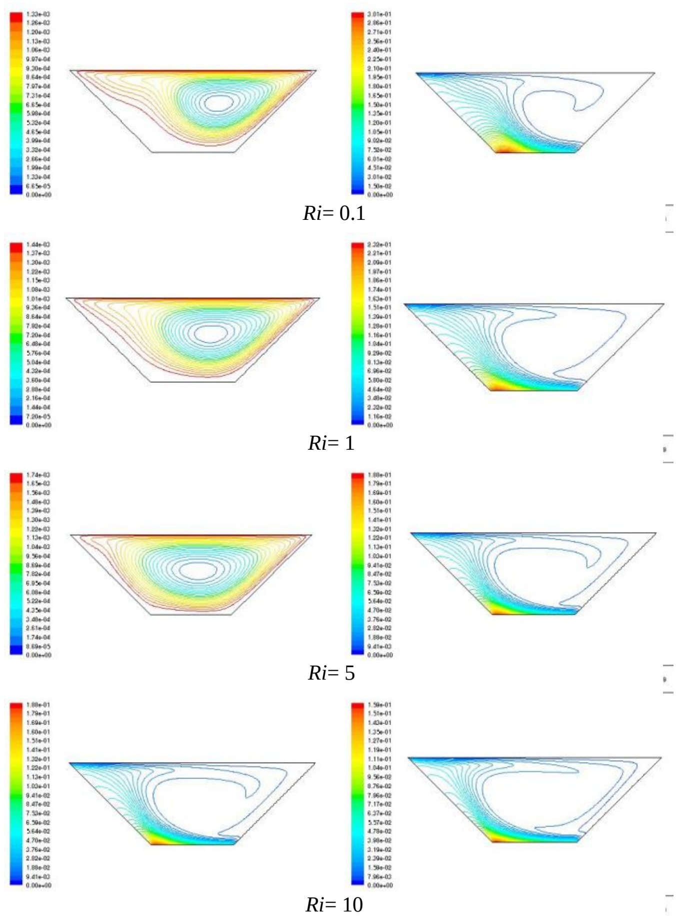

Figure 6: Contours of Streamlines and isotherms at Re=400, A=1.0 and γ=45°

From figure 8-9 the average value of the Nusselt number with respect to the Richardson number has been plotted. Here it can be seen that Nusselt number at γ=45º dominates the other two cases i.e. γ=30º and γ=60º, showing better heat transfer. So it is clearly visible that trapezoid having the inclination angle γ=45º gives better heat transfer and consequently it can be taken as the optimum inclination angle.

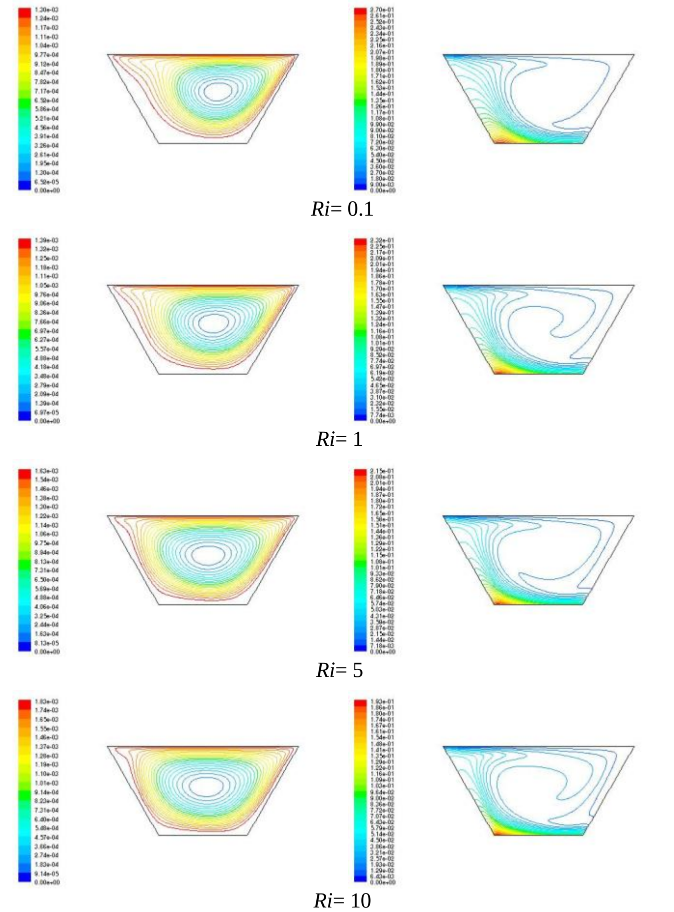

Figure 7: Contours of Streamlines and isotherms at Re=400, A=1.0 and γ=60°

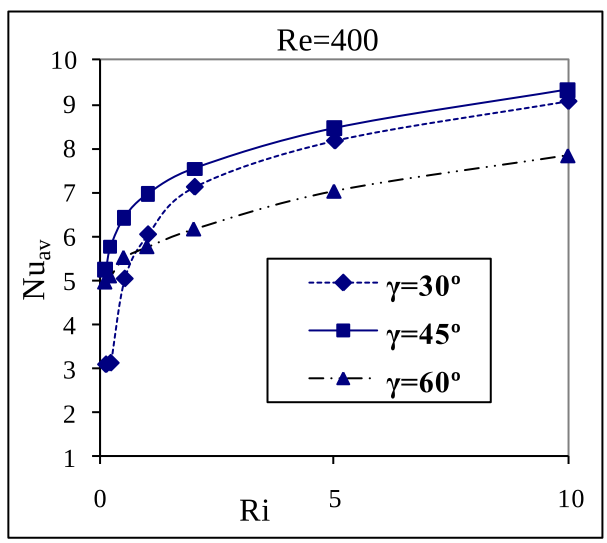

Figure 8: Average Nusselt number, Nu_{av} vs Richardson number at Re=400, A=1

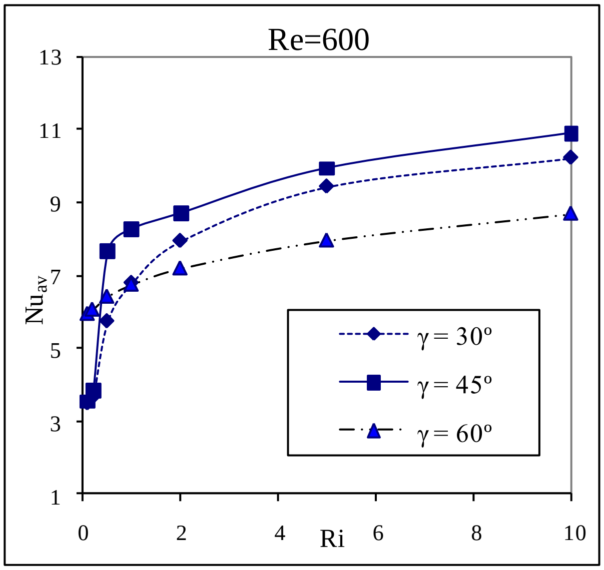

Figure 9: Average Nusselt number, Nu_{av} vs Richardson number at Re=600, A=1

3.2 Effect of rotational angle, Φ

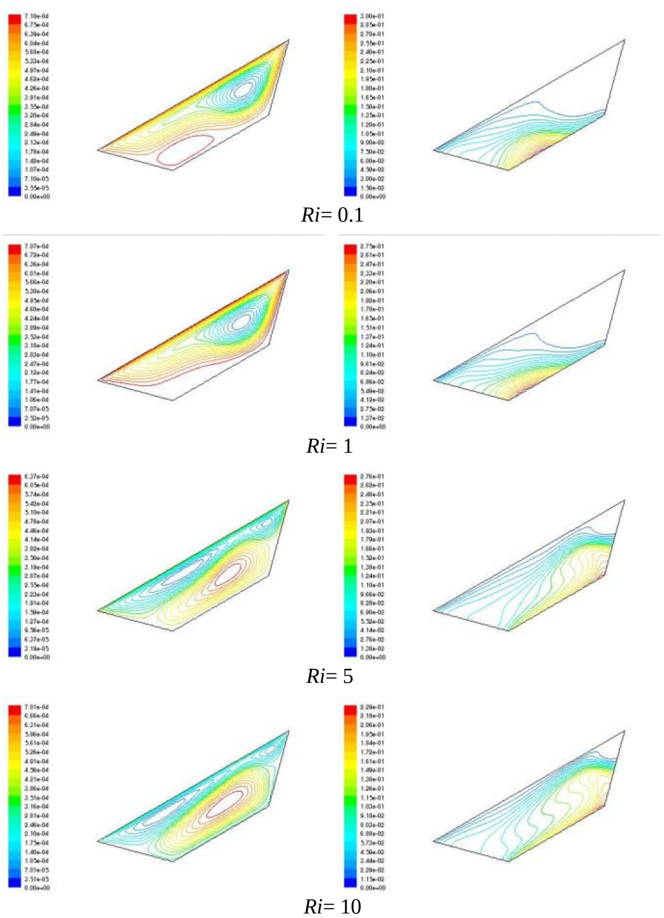

Figure 10: Contours of Streamlines and isotherms at Re=400, A=0.5 and Φ=30°, Opposing Flow

Next the effect of rotational angle, Φ has been studied. When studying the effect of rotational angel, two distinct cases have been taken into consideration. They are aiding and opposing flow condition. The first one is when the shear driven flow opposes the convective flow and in that case the top moving lid is moving in the positive direction at a specified rotational angle [figure 1]. The second condition is the aiding flow condition where the shear driven flow aids the natural convective flow and the moving top lid moves in the opposite direction unlike the first case [figure 2]. Both these cases have been studied for a rotational angle for Φ=30º, 45º and 60º and their heat transfer characteristics has been studied in terms of streamlines and isothermal plots.

Unlike Φ=0º, when the buoyancy is acting only in the y direction, as the rotational angle Φ changes, the flow field changes significantly. In opposing flow condition the shear driven flow opposes the natural convective flow, At low Richardson number (*Ri*<1)the forced convection is dominating, creating a single circulation at the right corner of the top moving lid [figure 10-12].

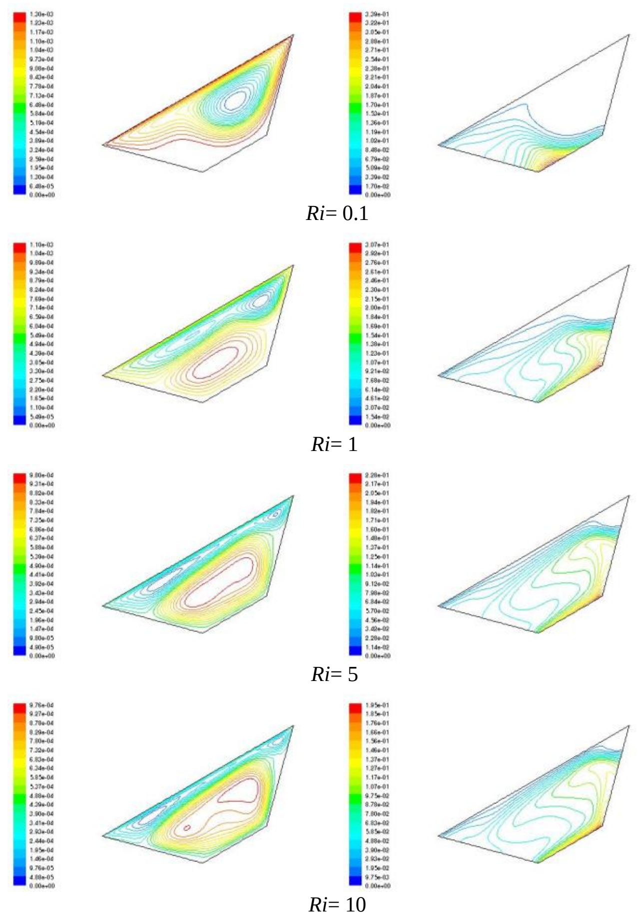

Figure 11: Contours of Streamlines and isotherms at Re=400, A=1 and Φ=30°, Opposing Flow

As the Richardson number increases (*Ri*>1), natural convection becomes dominating creating a large circulation at the bottom of the cavity. This large circulation causing by natural convection goes bigger and stronger as *Ri* number increases as well as squeezes the upper circulation, resulting an opposing effect. If we observe the isothermal plots, it changes accordingly with streamlines. As *Ri* number increases, the isothermal lines changes significantly indicating that the convection is the dominating heat transfer for the specified case. The shear driven circulation at the upper right side becomes smaller and smaller as the *Ri* number increases because of dominating natural convection.

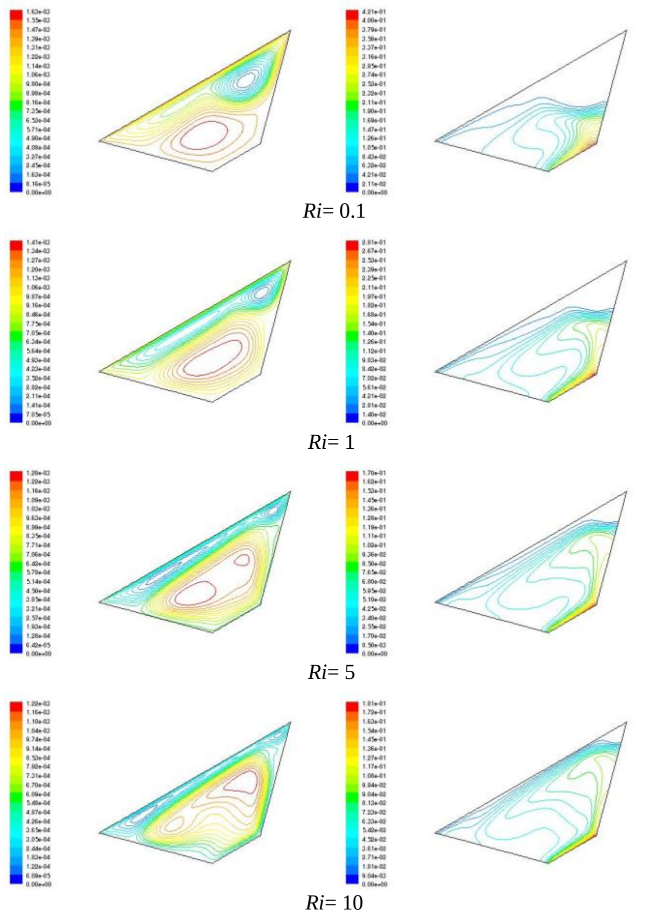

Figure 12: Contours of Streamlines and isotherms at Re=400, A=1.5 and Φ=30°, Opposing Flow

In the case of aiding flow, condition when the forced convection aids the natural convection a different scenario has been observed [e.g. figure 13]. In all the cases, a single circulation of the size of the cavity has been observed. Unlike the opposing flow condition, in that case the natural convection aids the shear driven flow from the smaller value of *Ri* number, resulting a much stronger convective current. As the *Ri* number increases, the convection flow fields become more and more stronger resulting better and better heat transfer. The isotherms changes significantly as the Richardson number increases and gives the minimum value at higher *Ri* number.

As the aspect ratio, *A* increases the convective flow fields become more and more stronger. As cavity volume increases with aspect ratio and more volume of cooling air is involved in cooling the heat source leading to better cooling effect. The effect of aspect ratio at different rotational angle has also been studied. In all the cases, it can be observed that Nu_{av} increases with increasing aspect ratio for all rotational angles, leading to better heat transfer.

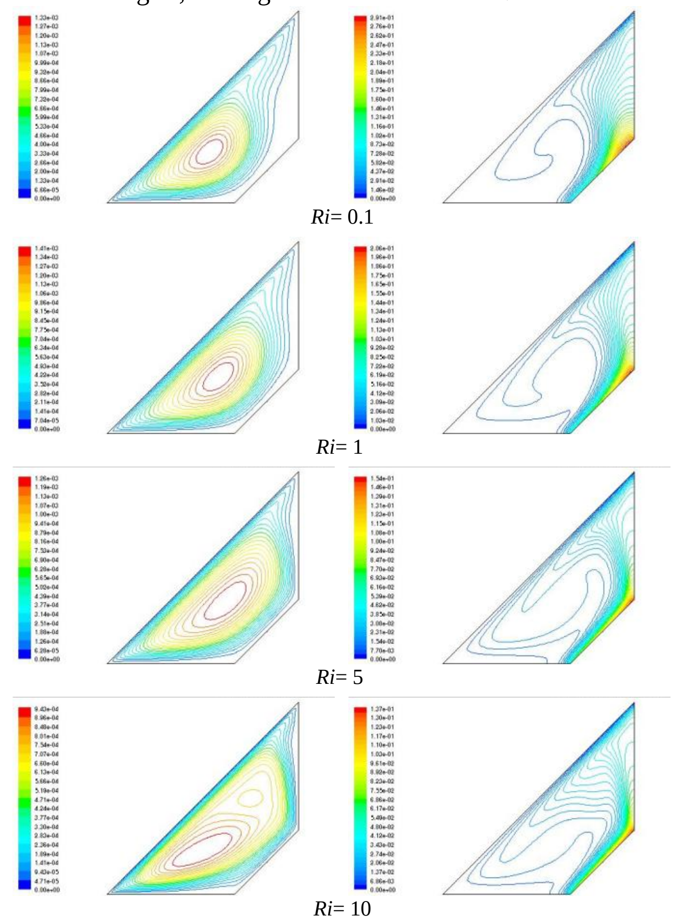

Figure 13: Contours of Streamlines and isotherms at Re=400, A=1 and Φ=45°, Aiding Flow

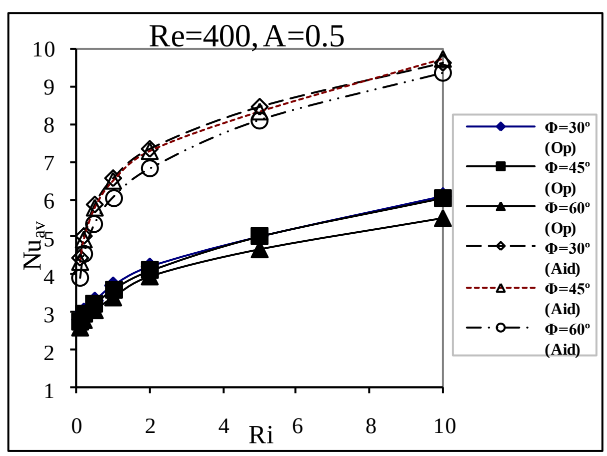

Figure 14: Variation of Nu_{av} with Ri at A=0.5, Re=400

Fig. 14-18 shows a comparative analysis of aiding and opposing flow conditions. There it can be seen that, the aiding flow condition always dominates the opposing flow condition in terms of Nu_{av} , which indicates better heat transfer at all rotational angle. The aiding flow condition provides stronger convective currents, which has been visible in the study, as the natural convection aids the shear driven flow. As a result the maximum value of the isotherms is lower in case of aiding flow condition, indicating lower temperature. But in opposing condition the natural convection opposes the shear driven flow, providing weak convective currents.

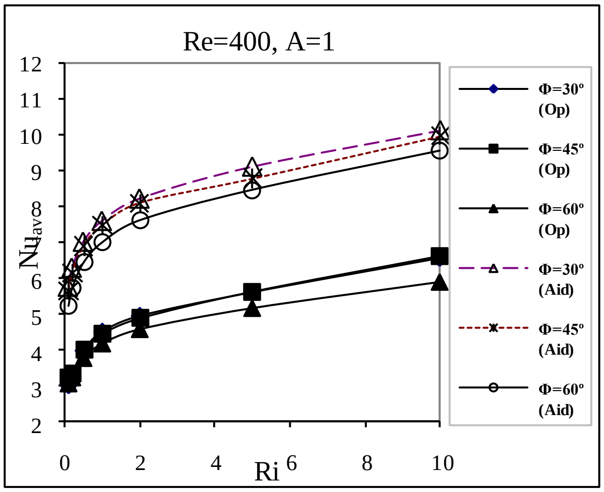

Figure 15: Variation of Nu_{av} with Ri at A=1, Re=400

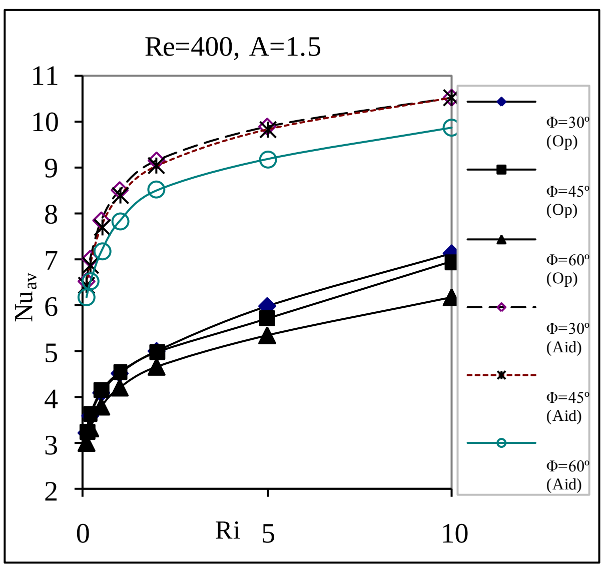

Figure 16: Variation of Nu_{av} with Ri at A=1.5, Re=400

The Nu_{av} is also sensitive to rotational angle, figure 14-18. At Re=400 it can be seen that, Nusselt number decreases as the rotational angle, Φ increases. Nu_{av} increases marginally at Φ=30º from Φ=45º but at Φ=60º, Nu_{av} drops significantly for all the aspect ratios, figure 14-17.The flow fields also changes accordingly. At *Re*=600, the maximum heat transfer has been obtained at Φ=45º, in terms of average Nusselt number, figure 18. Nu_{av} increases marginally at Φ=45º from Φ=30º but drops significantly at Φ=60º, indicating poor heat transfer at Φ=60º.

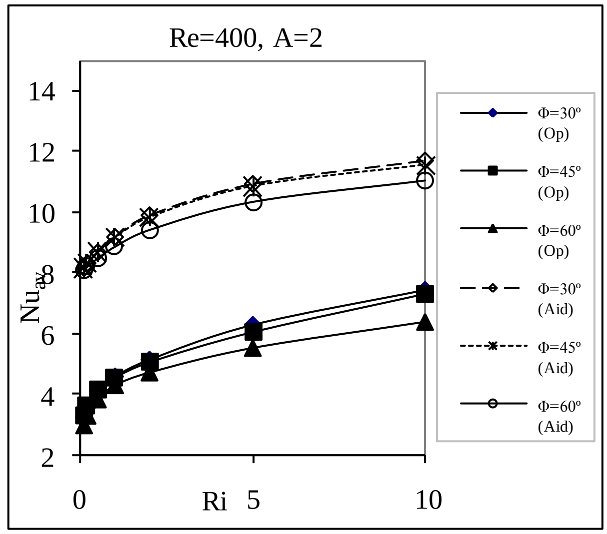

Figure 17: Variation of Nu_{av} with Ri at A=2, Re=400

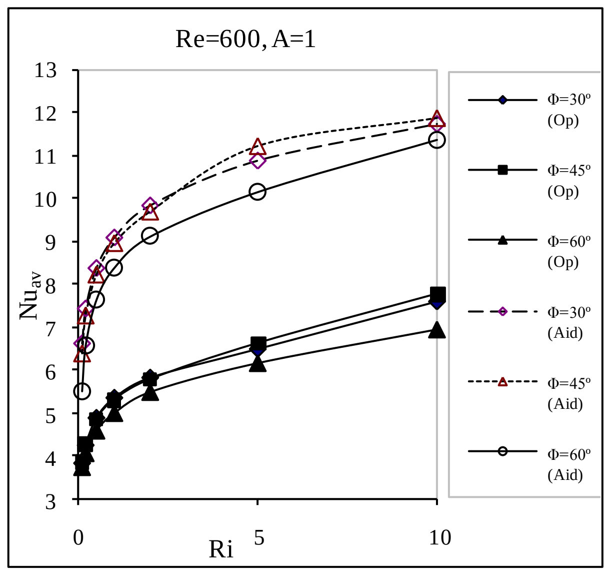

Figure 18: Variation of Nu_{av} with Ri at A=1, Re=600

3.3 Effect of Richardson number, *Ri*

The value of the Richardson number, $Ri=Gr/Re^2$ provides a measure of the importance of buoyancy driven natural convection relative to the lid driven forced convection. When the Buoyancy effects are relatively small, *Ri*<1, the gross flow features are similar to those of a conventional non-stratified fluid at comparable values of Re. The main circulation fills the entire cavity of the size of the cavity generated by the movement of the top wall. Minor cells may be visible near the bottom corners. The streamlines and isotherms indicated that the hydrodynamic and thermal boundary layers are not developed fully at low Richardson number. The isothermal lines are mostly undistorted and horizontal lines except the large recirculating area inside the cavity at low Richardson number. In the large recirculating zone temperature gradients are very weak. This implies that, due to the vigorous actions of the mechanically driven circulations, fluids are well mixed; consequently, temperature differences in much of this interior region are very small.

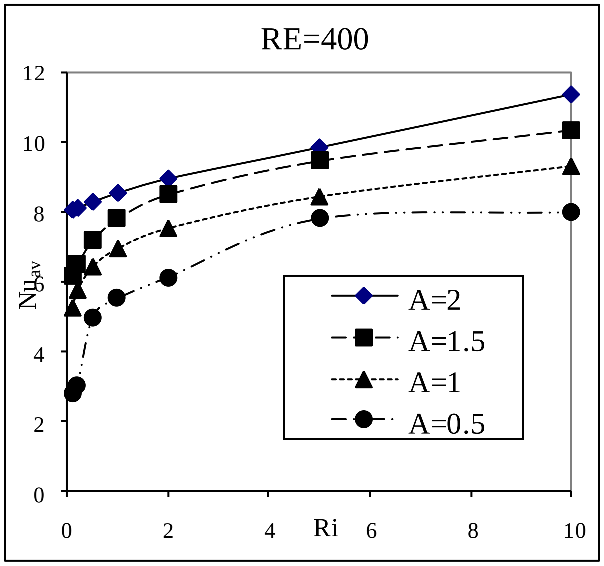

Figure 19: Variation of Nu_{av} with Ri at Re=400 and Φ=0º

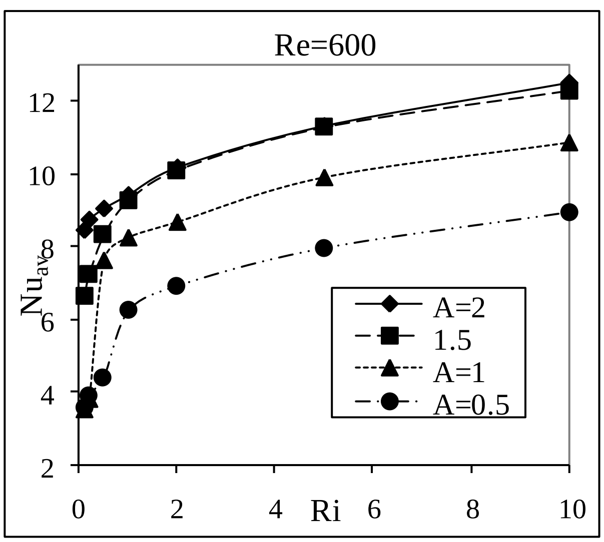

Figure 20: Variation of Nu_{av} with Ri at Re=600 and Φ=0º

When *Ri*>1, natural convection begins to dominate the forced convection. The Buoyancy assists the core flow and thus the convection current becomes more and more strong with increasing Richardson number. As Richardson number increases, the main circulation occupies the whole cavity and it become more symmetrical inside the cavity. If we see the isothermal plots, we can see that as the Richardson number increases the isothermal lines becomes more and more denser at the upper cold lid. The crowded streamlines and isothermal lines indicate that the hydrodynamic and thermal boundary layers have been developed along the hot wall and cold wall, respectively, reflecting rigorous heat transfer rate occurred. Consequently the maximum temperature reduces due to this large heat transfer rate.

The average Nusselt number as a function of Richardson number has been plotted in figure 19-20 for different Reynolds number. It can be observed that as the Richardson number increases the average Nusselt number increases accordingly for all the aspect ratios. When *Ri*<1 , Nu_{av} grows only slightly with increasing *Ri*. After *Ri* is more than 1, Nu_{av} is found to increase more rapidly. Since *Re* is kept constant the forced convection effect remains invariant as *Ri* increases for a particular case. When *Ri*>1, the natural convection aids more and more in the heat transfer process in addition to the forced convection which results in more rapid increase of Nu_{av}.

3.4 Effect of Aspect Ratio, *A*

Changing the aspect ratio, *A* (*A=H/W*) causes a change in heat transfer characteristics. In order to investigate the convection heat transfer at different aspect ratios, computations has been done for cavities at aspect ratios of 0.5, 1, 1.5 and 2.0. Keeping Reynolds number fixed at 400 and 600 the Richardson number has been changed from 0.1 to 10. If we compare the flow fields at different aspect ratios from 0.5 to 2.0, it can be revealed that in the convection region adjacent to the heat source, the isotherms become thinner and denser producing higher temperature gradients with increasing aspect ratio. The streamlines becomes stronger as the aspect ratio increases. This is due to the fact that the cavity volume increases with aspect ratio and more volume of cooling air is involved in cooling the heat source leading to better cooling effect.

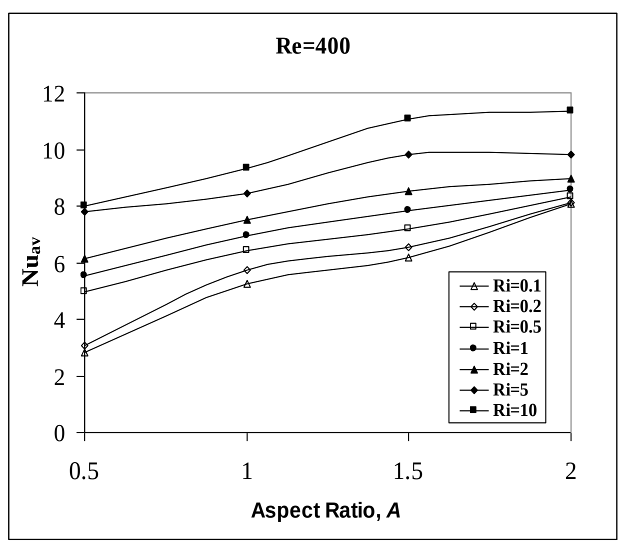

Figure 21: Variation of Nu_{av} with A at Re=400 and Φ=0º

The average Nusselt number at the heat source surface has been plotted in figure 21-22 for a range of *Ri* and aspect ratios. For a particular aspect ratio, the Nu_{av} increases with increasing *Ri*. As a result, the maximum temperature decreases monotonously which can be recognized from the isothermal plots. As the aspect ratio increases from 0.5 to 1 the Nu_{av} increases for a particular *Ri*.

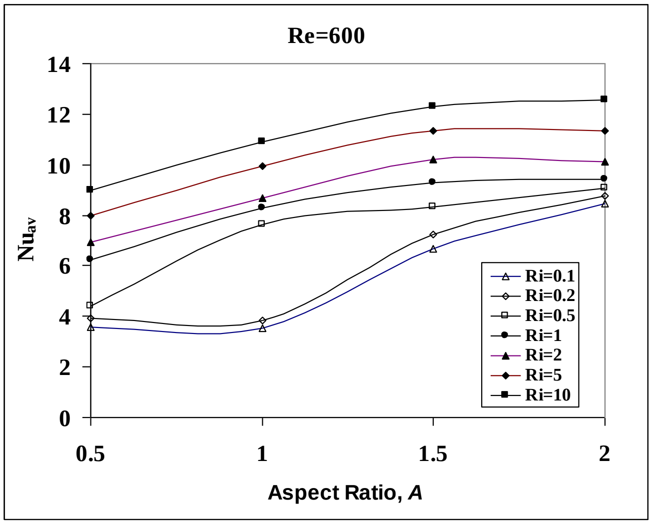

Figure 22: Variation of Nu_{av} with A at Re=600 and Φ=0º

At higher Reynolds number i.e. Re=600, with increasing aspect ratio some secondary eddy at the bottom surface of the cavity has been observed. This is of frictional losses and stagnation pressure. As the *Ri* increases, natural convection dominates more and the bottom secondary eddies blends into the main primary flow. For A>1.5 the variation is almost flat indicating that the aspect ratio does not play a dominant role on the heat transfer process at that range.

3.5 Effect of Reynolds number, *Re*

This study has been done at two different Reynolds numbers. They are Re=400 and Re=600. With a particular case keeping *Ri* and *A* constant, as the Reynolds number increases the convective current becomes more and more stronger and the maximum value of the isotherms reduces. As we know $Ri=Gr/Re^2$. *Gr* is square proportional of *Re* for a fixed *Ri*. So slight change of Re and *Ri* causes huge change of *Gr*. *Gr* increases the buoyancy force. As buoyancy force is increased then heat transfer rate is tremendously high. So changes are very visible to the change of *Re*. From figure 19-20, it can be observed that as the *Re* increases the average Nusselt number also increases for all the aspect ratios.

4. CONCLUSION

Two dimensional steady, mixed convection heat transfer in a two-dimensional trapezoidal cavity with constant heat flux from heated bottom wall while the isothermal moving top wall in the horizontal direction has been studied numerically for a range of Richardson number, Aspect ratio, the inclination angle of the side walls and the rotational angle of the cavity. A number of conclusions can be drawn from the investigations:

The optimum configuration of the trapezoidal enclosure has been obtained at γ=45º, as at this configuration the Nu_{av} was maximum at all Richardson number.

As the Richardson number increases the Nu_{av} increases accordingly at all Aspect ratios, because at higher Richardson number natural convection dominates the forced convection.

As Aspect Ratio increases from 0.5 to 2.0, the heat transfer rate increases. This is due to the fact that the cavity volume increases with aspect ratio and more volume of cooling air is involved in cooling the heat source leading to better cooling effect.

The direction of the motion of the lid also affects the heat transfer phenomena. Aiding flow condition always gives better heat transfer rate than opposing flow condition. Because at aiding flow condition, the shear driven flow aids the natural convective flow, resulting a much stronger convective current that leads to better heat transfer.

The Nu_{av} is also sensitive to rotational angle Φ. At Re=400 it can be seen that, Nusselt number decreases as the rotational angle, *Φ* increases. Nu_{av} increases marginally at Φ=30 from Φ=45º but at *Φ*=60º, Nu_{av} drops significantly for all the aspect ratios.

REFERENCES

Cha, C. K. and Jaluria, Y., 1984. Recirculating mixed convection flow for energy extraction, Int. J. Heat Mass Transfer, Vol. 27, pp.1801-1810.

Imberger, J. and Hamblin, P. F., 1982. Dynamics of lakes, reservoirs, and cooling ponds, A. Rev. FIuid Mech. Vol. 14, pp. 153-187.

Ideriah, F. J. K. , 1980. Prediction of turbulent cavity flow driven by buoyancy and shear, J. Mech. Eng. Sci. Vol. 22, pp. 287-295.

Pilkington, L. A. B. , 1959. Review lecture: The float glass process, Proc. R. Sot. Lond., IA 314, pp. 1-25.

Aydin, O. and Yang, W.J., 2000. Mixed convection in cavities with a locally heated lower wall and moving sidewalls, Numer. Heat Transfer, Part A, Vol. 37, pp. 695–710.

Shankar, P.N., Meleshko, V.V., and Nikiforovich, E.I., 2002. Slow mixed convection in rectangular containers, J. Fluid Mech. Vol. 471. pp. 203–217.

Oztop, H.F. and Dagtekin, I., 2004. Mixed convection in two-sided lid-driven differentially heated square cavity, Int. J. Heat Mass Transfer, Vol. 47, pp. 1761–1769.

Sharif, M. A. R., 2007. Laminar mixed convection in shallow inclined driven cavities with hot moving lid on top and cooled from bottom, Applied Thermal Engineering, Vol. 27, pp. 1036–1042.

Guo, G. and Sharif, M. A. R., 2004. Mixed convection in rectangular cavities at various aspect ratios with moving isothermal sidewalls and constant flux heat source on the bottom wall, Int. J. Thermal Sciences, Vol. 43, pp. 465–475.

Basak, T., Roy, S., Singh, S.K. and Pop, I., 2010. Analysis of mixed convection in a lid-driven porous square cavity with linearly heated side wall(s), Int. J. Heat Mass Transfer, Vol. 53, pp. 1819-1840.